UTSA

Drag Model for Assemblies of Non-Spherical Particles

Project Award Number DE-FE0031894

PI: Zhi-Gang Feng, Ph.D.
Mechanical Engineering
University of Texas at San Antonio (UTSA)

May 1, 2024

Outlines

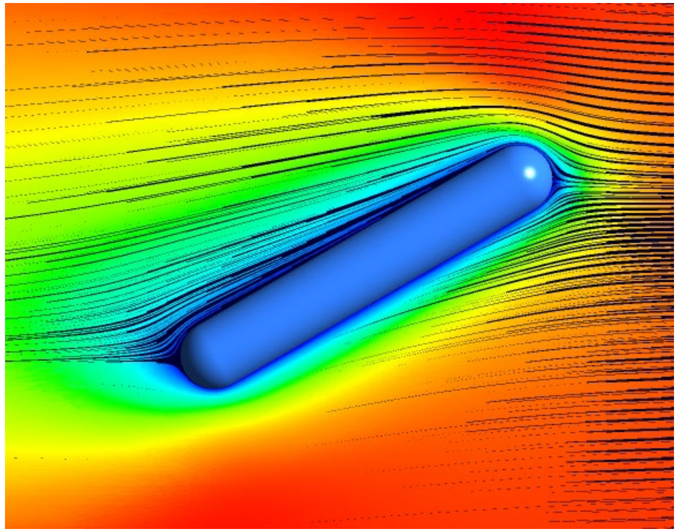

1. Introduction

2. Correlations of drag coefficients for individual non-spherical particles

3. Artificial Neural Network (ANN) models for individual non-spherical particles

4. Drag models for assemblies of non-spherical particles

5. Future Work

Importance of Research

Particle hydrodynamic forces exerted on particles play a pivotal role in particulate flow simulation packages

Many particles in the real world are non-spherical, with ellipsoids and spherocylinders being among the most common shapes.

Developing a more precise model tailored to non-spherical particles could improve the accuracy of particulate flow simulations.

The applications span a wide array of fields, from biological systems to industrial processes.

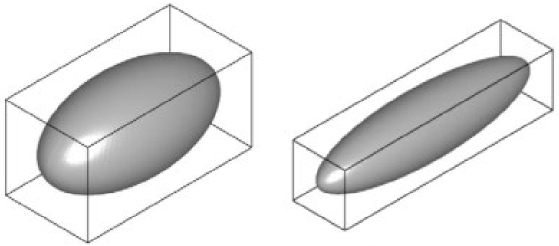

Dispersion of Pollutants

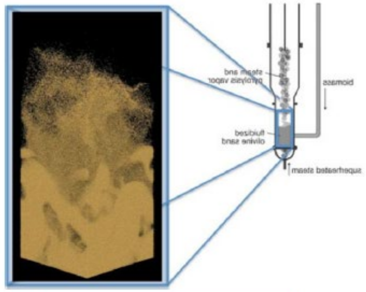

Coal Combustion

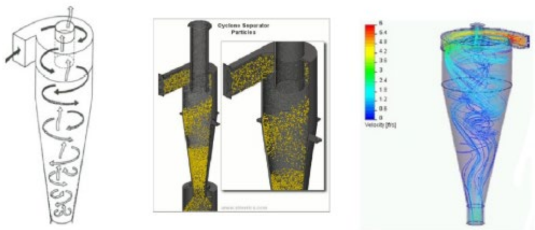

Separation Process (cyclone)

Technical background

- Research on non-spherical particle drag is scarce in the literature.
- Existing particulate simulation packages operate under the assumption that particles are spherical, employing spherical drag force models.
- Drag could differ significantly between spherical particles and non-spherical particles

Gidaspow drag correlation

$$\beta_{gm} = \begin{cases} \frac{3}{4} C_D \frac{\rho_g \varepsilon_g \varepsilon_m \left|\mathbf{u}_g - \mathbf{u}_m\right|}{d_{pm}} \varepsilon_g^{-2.65} & \varepsilon_g \geq 0.8 \\ \frac{150\varepsilon_s\left(1-\varepsilon_g\right)\mu_g}{\varepsilon_g d_{pm}^2} + \frac{1.75\rho_g \varepsilon_m \left|\mathbf{u}_g - \mathbf{u}_m\right|}{d_{pm}} & \varepsilon_g < 0.8 \end{cases}$$

$$C_D = \begin{cases} 24/\mathrm{Re}\left(1+0.15\,\mathrm{Re}^{0.687}\right) & \mathrm{Re} < 1000 \\ 0.44 & \mathrm{Re} \geq 1000 \end{cases}$$

$$\mathrm{Re} = \frac{\rho_g \varepsilon_g \left|\mathbf{u}_g - \mathbf{u}_m\right| d_{pm}}{\mu_g}$$

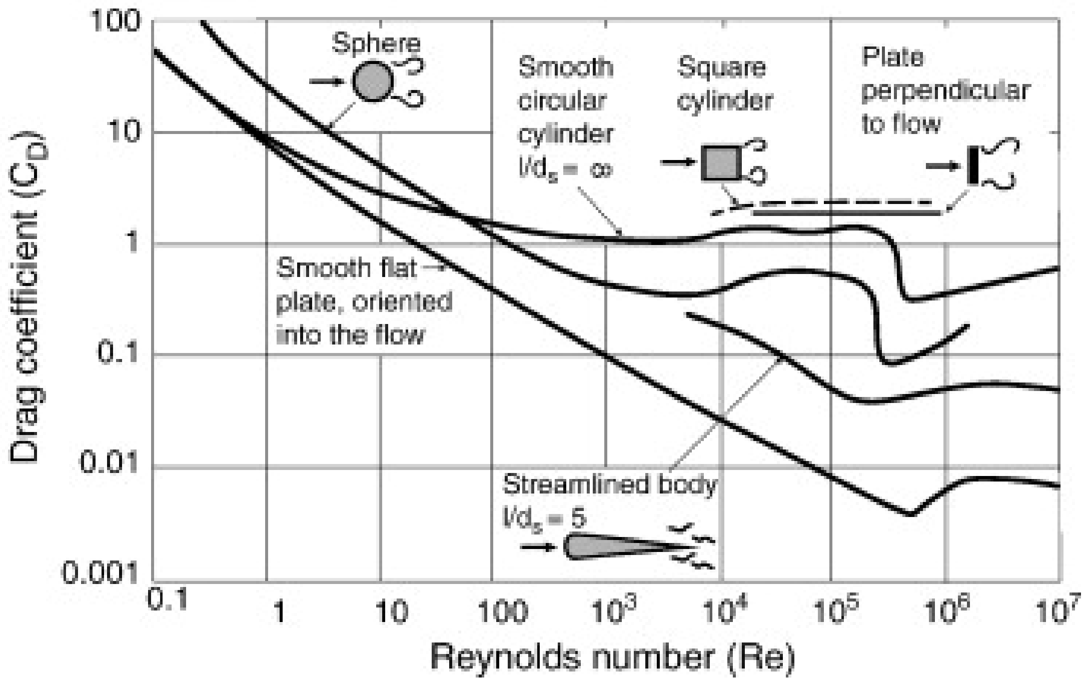

Descriptions of a Non-spherical Particle

.

(5)

The “Size” of non-spherical particles

The volume equivalent diameter: $d_V = \sqrt[3]{\frac{6V}{\pi}}$

The longest dimension of the particle, L_L.

The shortest dimension of the particle, L_S.

An intermediate dimension of the particle, L_I, typically defined as $(L_L L_S)^{0.5}$.

The diameter of the smallest sphere that circumscribes the particle, d_c.

The diameter of the largest sphere that may be enclosed by the particle, d_e.

The "Shape" of a non-spherical particle

The sphericity: defined as the ratio of the surface area of the sphere with equivalent volume to the actual surface area of the particle

Corey shape factor: primarily used for ellipsoids with three semi-axes a>b>c: $\beta = \frac{c}{\sqrt{ab}}$

Circularity (roundness): the ratio of the area equivalent diameter to the projected perimeter diameter of the particle in the direction of motion

***Aspect ratio* or *elongation*, E_L : defined as the ratio of its longest to its shortest dimension, L_L/L_S**

The *flatness* of a particle, F_L : defined as the ratio L_S/L_I. The size of the dimension L_I is between the longest and the shortest dimensions: $L_L > L_I > L_S$.

Drag Correlations of A Single Non-Spherical Particle

Spherical particle

Schiller and Nauman $C_D = \frac{24}{Re}\left(1+0.15Re^{0.687}\right)$

Clift and Gauvin $C_D = \frac{24}{Re}\left(1+0.15Re^{0.687}\right)+\left(\frac{0.42}{1+42500Re^{-1.16}}\right).$

Non-spherical particle

Haider & Levenspiel, 1989	$C_D = \frac{24}{Re}(1+ARe^B)+\frac{C}{1+\frac{D}{Re}}.$ $A = e^{2.3288-6.458\Phi+2.4486\Phi^2},$ $B = 0.0964+0.5565\Phi,$ $C = e^{4.905-13.8944\Phi+18.4222\Phi^2-10.2599\Phi^3},$ $D = e^{1.4681+12.2584\Phi-20.7322\Phi^2+15.8855\Phi^3}.$
Swamee & Ojha, 1991	$C_D = 0.84\left[\frac{33.78}{(1+4.5\beta^{0.35})^{0.7}Re^{0.56}}+\left(\frac{Re}{Re+700+1000\beta}\right)^{0.28}\frac{1}{(\beta^4+20\beta^{20})^{0.175}}\right]^{1.428}.$ $\beta = \frac{c}{\sqrt{ab}}$ is the Corey shape factor, where a, b, and c = lengths of the three principal axes of the particle in decreasing order of magnitude.
Ganser, 1993	$C_D = \frac{24}{ReK_1}[1+0.1118(ReK_1K_2)^{0.6567}]+\frac{0.4305K_2}{1+\frac{3305}{ReK_1K_2}}.$ $K_1 = \left(\frac{1}{3}+\frac{2}{3\sqrt{\Phi}}\right)^{-1}$ for isometric-like particles or $K_1 = \left(\frac{d_{PA}}{3d_V}+\frac{2}{3\sqrt{\Phi}}\right)^{-1}$ for non-isometric-like particles. d_{PA} is the diameter of the equal projected circular area. $K_2 = 10^{1.8148(-\log\Phi)^{0.5743}}.$
Chien, S. F., 1994.	$C_D = \frac{30}{Re}+67.289e^{-5.03\Phi}.$
Tran-Cong, et al. , 2004	$C_D = \frac{24}{Re\frac{d_{PA}}{d_V}}\left[1+\frac{0.15}{\sqrt{c_P}}\left(Re\frac{d_{PA}}{d_V}\right)^{0.687}\right]+\frac{0.42}{\sqrt{c_P}\left[1+4.25\times10^4\left(Re\frac{d_{PA}}{d_V}\right)^{-1.16}\right]}.$ The *projected area diameter* defined as the diameter of a circle that would have the same area projected in the direction of the motion the particle $d_{PA} = \sqrt{\frac{4A_P}{\pi}}.$ The *projected circularity*, is the ratio of the perimeter of the projected circle in the direction of motion to the actual perimeter of the particle projected in the same direction: $c_P = \frac{\pi d_{PA}}{P} = \frac{\sqrt{4\pi A_P}}{P}.$

Loth, 2008	K_1 is chosen as $K_1 = \left(\frac{LI}{S^2}\right)^{-0.09}$ in the Ganser (1993) correlation.
Hölzer and Sommerfeld, 2008	$C_D = \frac{8}{Re\sqrt{\Phi_{\parallel}}}+\frac{16}{Re\sqrt{\Phi}}+\frac{3}{\sqrt{Re}\Phi^{\frac{3}{4}}}+\frac{0.4210^{0.4(-\log\Phi)^{0.2}}}{\Phi_T}.$ Often time $\Phi_{\parallel}$ is substituted by Φ_T for convenience.
Dioguardi, F., and Mele, 2015	$C_D = C_{Ds}\frac{1}{Re^2\Psi^a}\left(\frac{Re}{1.1833}\right)^{2.0721}, a = Re^{-0.23}\ for\ Re < 50\ and\ Re^{0.05}\ for\ 50 < Re \le 10^4.$ The modified sphericity factor $\Psi = \Phi/X.$
Bagheri & Bonadonna, 2016	$C_D = \frac{24K_S}{Re}\left[1+0.125\left(\frac{ReK_N}{K_S}\right)^{0.667}\right]+\frac{0.46K_N}{1+\frac{5330}{ReK_N/K_S}}, Re < 3\times10^5.$ $K_S = \frac{1}{2}\left(F_S^{\frac{1}{3}}+F_S^{-\frac{1}{3}}\right), K_N = 10^{a[-\log(F_N)]^b}$ with $a = 0.45+\frac{10}{e^{2.5(\log(\rho'))+30}}$ and $b = 1-\frac{37}{e^{3\log(\rho')+100}}$, and $F_S = fe^{1.3}\frac{d_V^3}{L_L L_I L_S}$ and $F_N = f^2e\frac{d_V^3}{L_L L_I L_S}$, where flatness $f = \frac{L_S}{L_I}$ and elongation $e = \frac{L_I}{L_L}.$

Non-Spherical Particles Implemented in the DNS Code

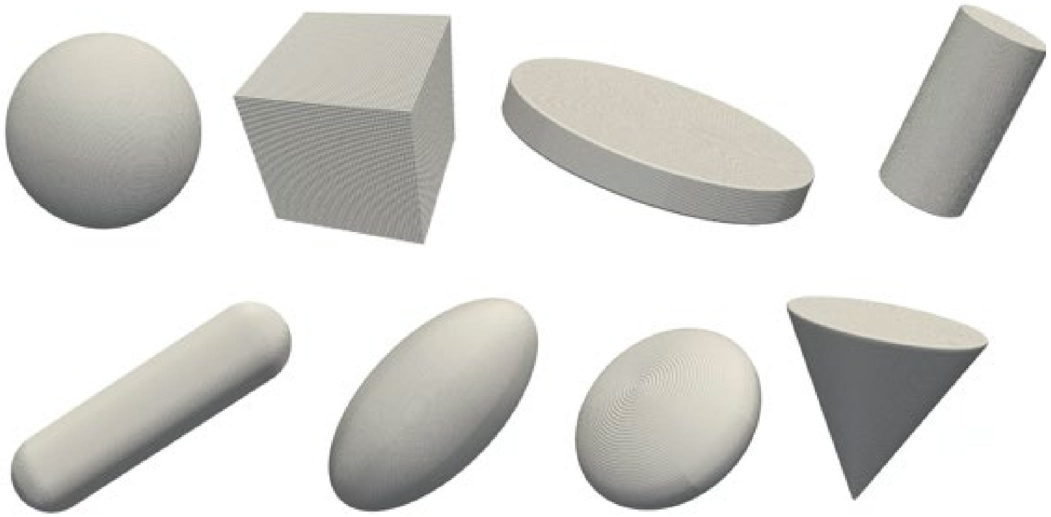

Particle Shape (r is radius, h is height)	d_V	A_P	$\mathbf{d_A}$	L_L	L_I	L_S	Φ
Sphere (r= a)	$2a$	$4\pi a^2$	$2a$	$2a$	$2a$	$2a$	1
Cube (side length a)	$1.241a$	$6a^2$	$\sqrt{6/\pi}a$	$\sqrt{3}a$	$\sqrt{2}a$	a	0.806
Disk (r=a, h=0.2a)	$1.063a$	$2.4\pi a^2$	$1.55a$	$2.01a$	$0.2a$	$0.2a$	0.471
Cylinder (r=a, h=4a)	$2.884a$	$10\pi a^2$	$3.31a$	$4.47a$	$4a$	$4a$	0.832
Spherocylinder (r=a, h=8a)	$3.530a$	$16\pi a^2$	$4a$	$8a$	$2a$	$2a$	0.779
Prolate (a=b, c=2a)	$2.520a$	$6.831\pi a^2$	$2.614a$	$4a$	$2a$	$2a$	0.930
Oblate (a=b, c=0.5a)	$1.587a$	$2.763\pi a^2$	$1.662a$	$2a$	$2a$	a	0.912
Cone (r=a, h=2a)	$1.587a$	$3.236\pi a^2$	$1.799a$	$2.236a$	$2a$	$2a$	0.778

Uniform flow over a Spherocylinder

- **Three Dimensionless Parameters - Inputs**
  - Reynolds Number: $Re = \frac{\rho U D_e}{\mu}$
  - Aspect ratio: $\beta = \frac{a+b}{a}$
  - Incident angle: θ
- **Three Coefficients - Outputs**
  - Drag coefficient: C_D
  - Lift coefficient: C_L
  - Torque coefficient: C_T

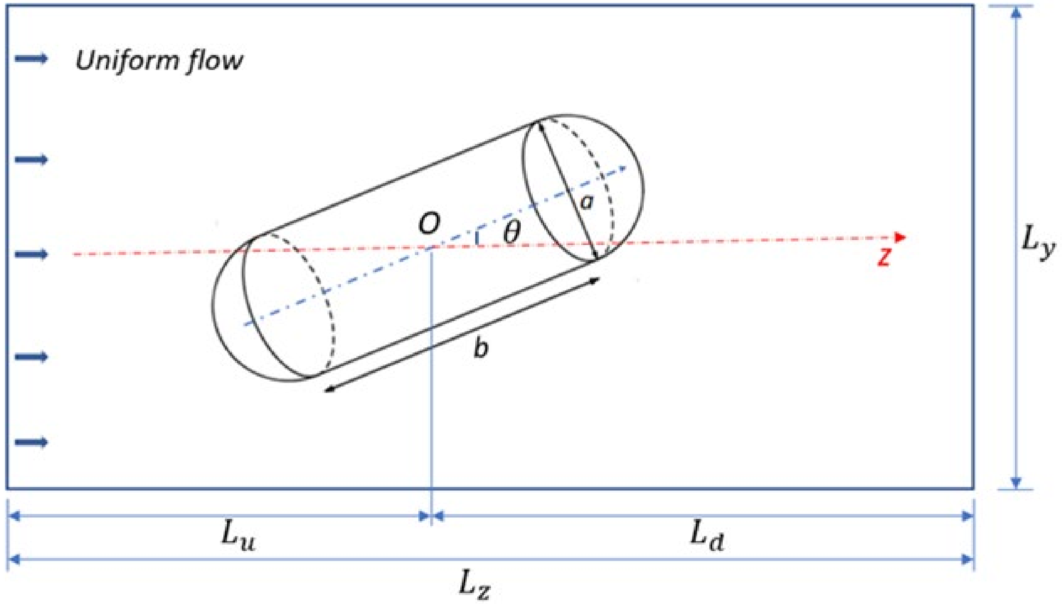

Simulation domain size and grid resolutions study

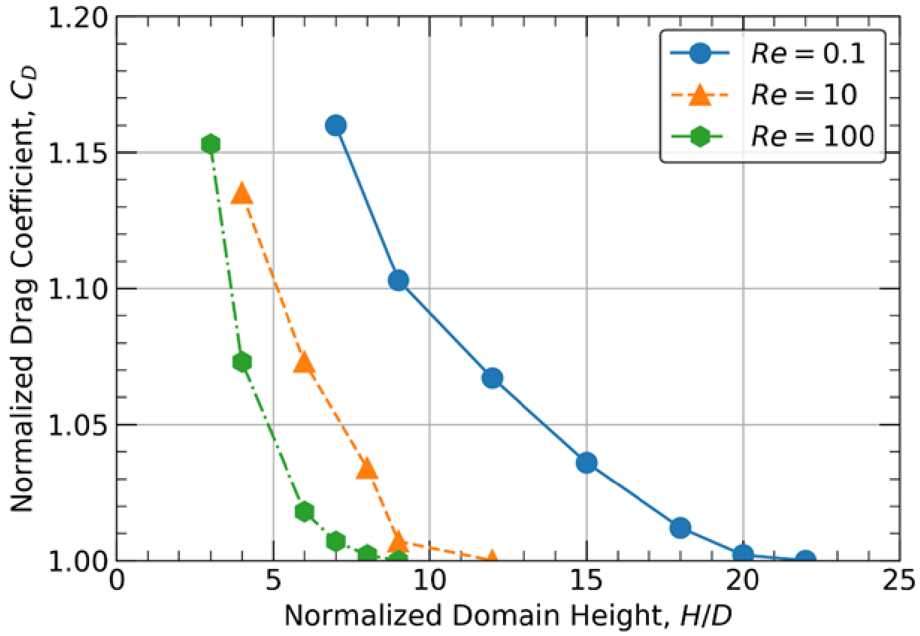

Affect of the domain size to the drag

Re	Grid Resolution (D/h)	Domain Size (L/D)
$0.1 \le Re \le 5$	10	$18 \times 18 \times 18$
$5 < Re \le 200$	20	$9 \times 9 \times 20$
$200 < Re$	30	$8 \times 8 \times 24$

Selection of grid resolution and grid size in the simulations

Validations

Drag Coefficient of a Sphere

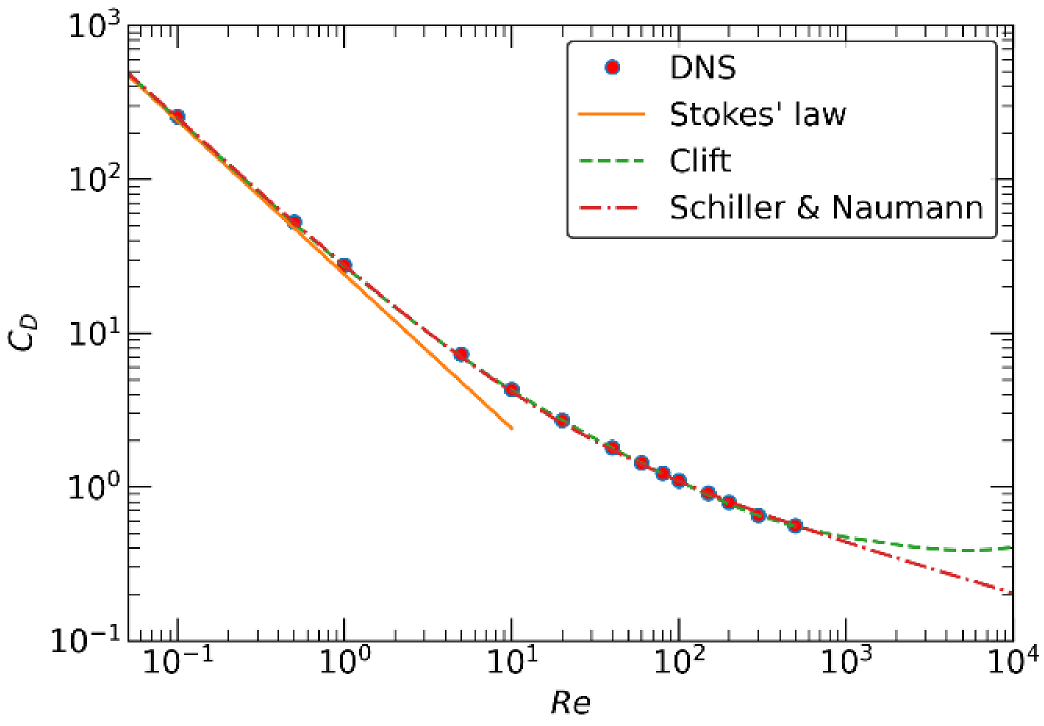

Spherocylinder at $\beta = 6$ and $\theta = \pi/3$

Re=10	C_D	C_L	C_T
Zastawny et al.	5.00	0.85	1.2
Ouchene	6.60	1.20	1.50
Present	6.92	1.23	1.57

Re=300	C_D	C_L	C_T
Zastawny et al.	1.25	0.56	0.6
Ouchene	1.49	0.56	0.84
Present	1.40	0.53	0.82

Correlation of Drag Coefficients of A Spherocylinder

Correlation of Drag Coefficient

- **Aspect Ratio:** $1 \le \beta \le 6$,
- **Orientation Angle:** $0^0 \le \theta \le 90^0$
- **Reynolds Number:** $0.1 \le Re \le 300$

$$C_{D,\theta} = C_{D,\theta=0^\circ} + (C_{D,\theta=0^\circ,90^\circ} - C_{D,\theta=0^\circ}) sin^n\theta$$

$$n = 2 - (0.72 - 0.062\beta)(1 - e^{-(0.012-0.0034\beta+0.00038\beta^2)Re}$$

$$C_{D,\theta=0^\circ} = (a_0 + a_1\beta^{0.5} + a_2\beta + a_3\beta^{1.5} + 0.15\beta^2)C_{Ds}$$

$$C_{D,\theta=90^\circ} = (b_0 + b_1\beta^{0.5} + b_2\beta + b_3\beta^{1.5} + 0.15\beta^2)C_{Ds}$$

$$a_0 = 2.460 + 0.203\sqrt{Re} - 0.00613Re.$$

$$a_1 = -3.461 - 0.324\sqrt{Re} + 0.00912Re.$$

$$a_2 = 2.957 + 0.151\sqrt{Re} - 0.00420Re.$$

$$a_3 = -1.084 - 0.0252\sqrt{Re} + 0.000699Re.$$

$$b_0 = 2.107 + 0.00357\sqrt{Re} - 0.00304Re.$$

$$b_1 = -3.037 - 0.0487\sqrt{Re} + 0.00575Re.$$

$$b_2 = 2.872 + 0.0605\sqrt{Re} - 0.00388Re.$$

$$b_3 = -1.070 - 0.0106\sqrt{Re} + 0.000641Re.$$

Results of General Drag Correlation*

Comparisons of Correlations
(Drag coefficient at $\theta = 0^o$ and $90^0$for $\beta = 4$)

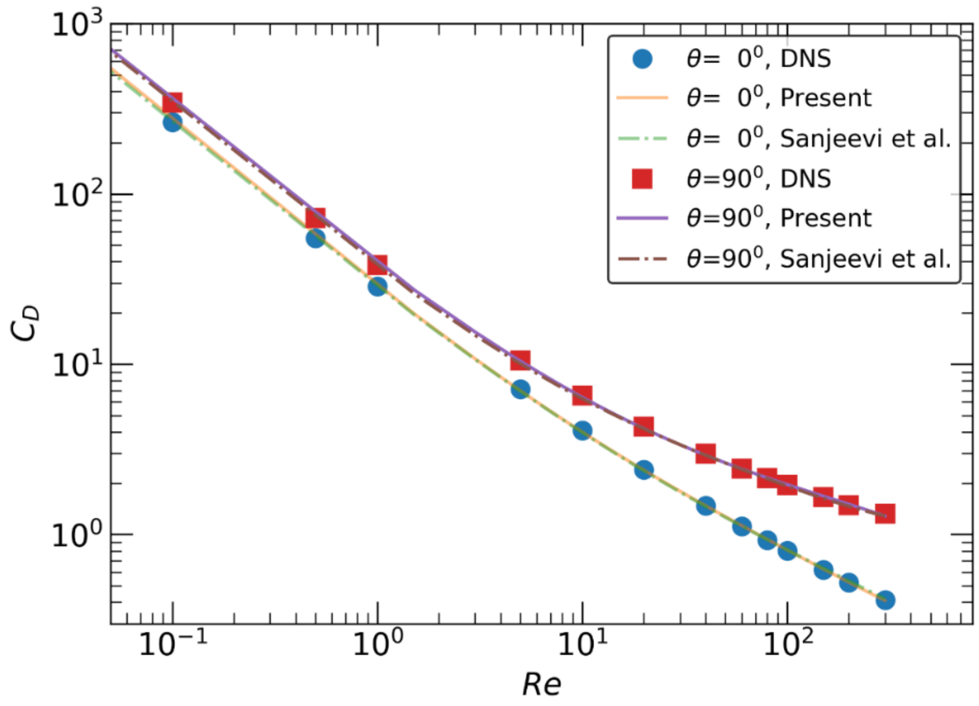

Drag coefficients for a spherocylinder in terms of (θ, β, *Re*)

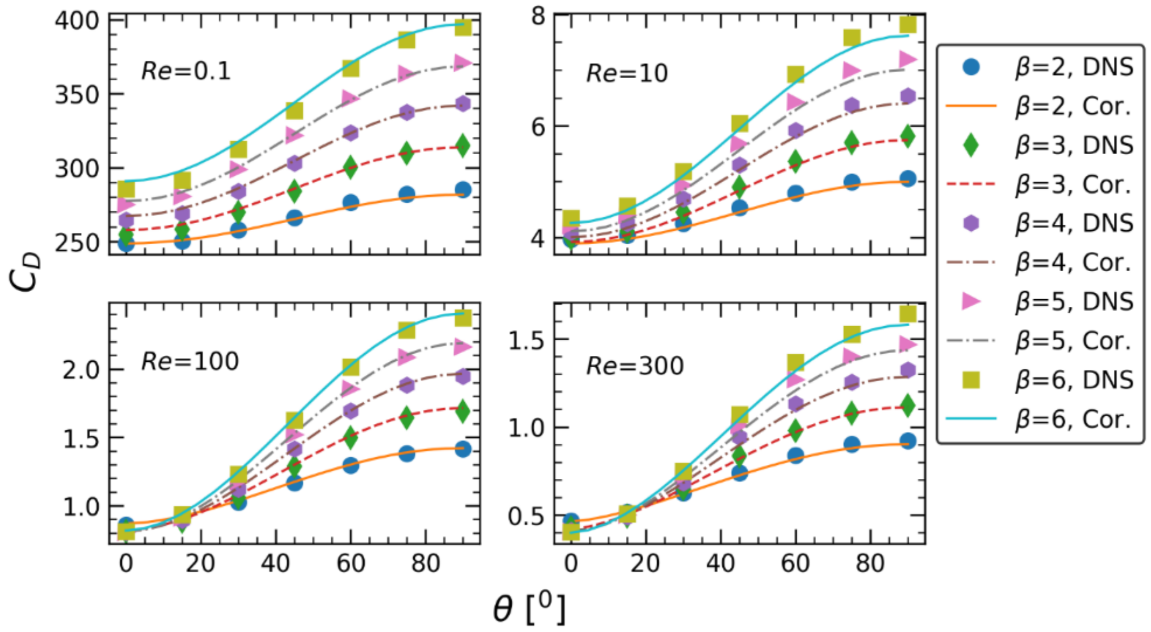

Correlation of Drag Coefficients of An Ellipsoid

Drag coefficient of an oblate

- **Aspect Ratio:** $0.1 \le \beta < 1$,
- **Orientation Angle:** $0^0 \le \theta \le 90^0$
- **Reynolds Number:** $0.1 \le Re \le 300$

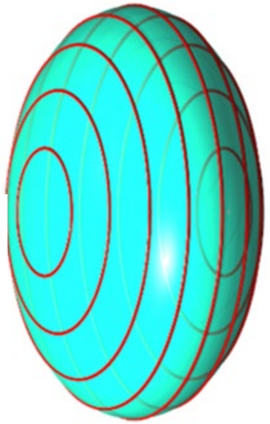

$$a_0 = 5.049 + 0.219\sqrt{Re} + 0.6841Re - 0.10133Re^{1.5} + 0.00374Re^2$$

$$a_1 = -16.408 + 0.723\sqrt{Re} - 4.2139Re + 0.64318Re^{1.5} - 0.023929Re^2$$

$$a_2 = 29.581 - 6.259\sqrt{Re} + 10.4596Re - 1.59645Re^{1.5} + 0.059298Re^2$$

$$a_3 = -26.511 + 10.481\sqrt{Re} - 11.5757Re + 1.7501Re^{1.5} - 0.064775Re^2$$

$$a_4 = 9.407 - 5.286\sqrt{Re} + 4.7065Re - 0.70377Re^{1.5} + 0.025962Re^2$$

$$C_{D,\theta} = C_{D,\theta=0°} + (C_{D,\theta=0°,90°} - C_{D,\theta=0°})sin^n\theta$$

$$C_{D,\theta=0°} = (a_0 + a_1\beta^{0.5} + a_2\beta + a_3\beta^{1.5} + a_4\beta^2)C_{Ds}$$

$$C_{D,\theta=90°} = (b_0 + b_1\beta^{0.5} + b_2\beta + b_3\beta^{1.5} + b_4\beta^2)C_{Ds}$$

$$b_0 = 3.306 + 0.673\sqrt{Re} - 0.1496Re + 0.01182Re^{1.5} - 0.000297Re^2$$

$$b_1 = -9.711 - 4.323\sqrt{Re} + 0.9641Re - 0.07901Re^{1.5} + 0.002032Re^2$$

$$b_2 = 16.492 + 10.062\sqrt{Re} - 2.2856Re + 0.19106Re^{1.5} - 0.004971Re^2$$

$$b_3 = -13.145 - 10.273\sqrt{Re} + 2.3737Re - 0.20098Re^{1.5} + 0.005274Re^2$$

$$b_4 = 4.112 + 3.871\sqrt{Re} - 0.9036Re + 0.07712Re^{1.5} - 0.002038Re^2$$

Correlation of Drag Coefficients of An Ellipsoid

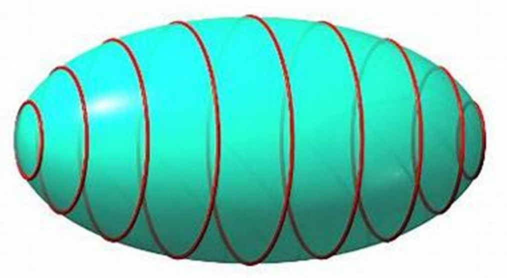

Drag coefficient of a prolate

- **Aspect Ratio:** $1 \leq \beta \leq 3$,
- **Orientation Angle:** $0^0 \leq \theta \leq 90^0$
- **Reynolds Number:** $0.1 \leq Re \leq 300$

$$C_{D,\theta} = C_{D,\theta=0^\circ} + (C_{D,\theta=0^\circ,90^\circ} - C_{D,\theta=0^\circ})sin^n\theta$$

$$C_{D,\theta=0^\circ} = (a_0 + a_1\beta^{0.5} + a_2\beta + a_3\beta^{1.5} + 0.35\beta^2)C_{Ds}$$

$$C_{D,\theta=90^\circ} = (b_0 + b_1\beta^{0.5} + b_2\beta + b_3\beta^{1.5} + 0.5\beta^2)C_{Ds}$$

$$a_0 = 2.993 + 0.2841\sqrt{Re} - 0.00961Re$$

$$a_1 = -5.026 - 0.5279\sqrt{Re} + 0.01813Re$$

$$a_2 = 4.799 + 0.3082\sqrt{Re} - 0.01113Re$$

$$a_3 = -2.087 - 0.063\sqrt{Re} + 0.00235Re$$

$$b_0 = 3.020 - 0.0196\sqrt{Re} + 0.00159Re$$

$$b_1 = -5.862 - 0.0026\sqrt{Re} - 0.00423Re$$

$$b_2 = 6.239 + 0.0241\sqrt{Re} + 0.00355Re$$

$$b_3 = -2.868 - 0.0005\sqrt{Re} - 0.00118Re$$

Limitations of Correlations

1.These methods are primarily designed for analyzing relationships between two variables, making it challenging to extend them to handle three or more variables effectively.

2.Correlations are highly sensitive to outliers in the data, often resulting in skewed and inaccurate results.

3.Risk of overfitting, where the model fits the training data too closely and performs poorly when applied to new, unseen data.

4. Unable to develop accurate correlations for lift and torque coefficients due to the intricate nature of the particle shapes a

Completed Master Thesis:

1. Joshua Conner (2022), “Prediction of the flow dynamics of a sphere translating near a plane wall using a muti-output deep learning model.”

2. Sergio Molina (2023), “Implementing artificial neural networks to estimate coefficients of drag, lift, and torques of spherocylinder particles.”

3. Daniel Hinojosa (2024), “Using an artificial neural network to predict the drag, lift and torque coefficients of an ellipsoid in a viscous fluid.”

Ongoing Doctoral Dissertation:

Jack Smith (expected completion in 2025), “Developing artificial neural network models for assemblies of non-spherical particles.”

Neural Network Model for An Spherocylinder

Collect Data

- 1200 data points generated via Direct Numerical Simulations (DNS)
- Input features:
  - Aspect Ratio, β: [1.0 – 6.0]
  - Reynolds Number, Re: [0.1 – 300]
  - Angle of Incident, θ : [0° – 90°]
- Output features:
  - Coefficient of Drag, C_D: [0 – 400]
  - Coefficient of Lift, C_L: [0 – 60]
  - Coefficient of Torque, C_T: [0 – 6]

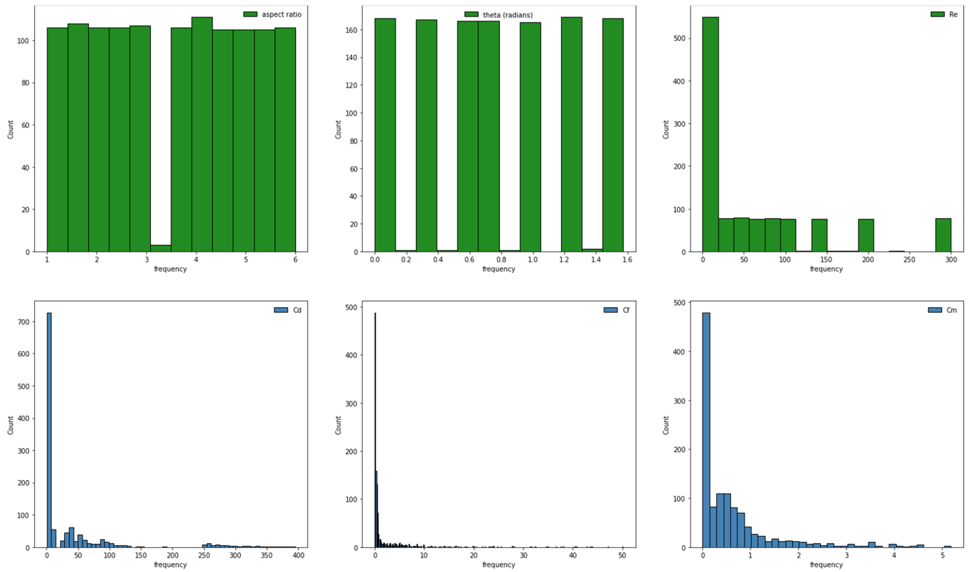

Neural Network Model for An Spherocylinder

Distributions in Data

- The output label data is right-skewed, exponentially distributed
- Skewed distributions lead to model learning bias due to over-representation
- The range of values is large which can also result learning bias towards larger values
  - Coefficient of Drag, C_D: [0 – 400]
  - Coefficient of Lift, C_L: [0 – 60]
  - Coefficient of Torque, C_T: [0 – 6]

Data Preprocessing

- Data transformation via Box-Cox transformation
  - $x_{trans} = \begin{cases} \frac{x^\lambda}{\lambda}, & \lambda \neq 0 \\ \ln(x+1), & \lambda = 0 \end{cases}$
  - $y_{trans} = \begin{cases} \frac{y^\lambda}{\lambda}, & \lambda \neq 0 \\ \ln(y+1), & \lambda = 0 \end{cases}$
  - λ set to 0.25

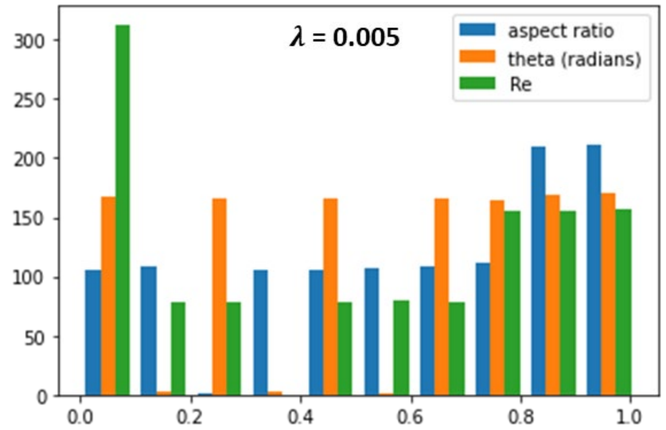

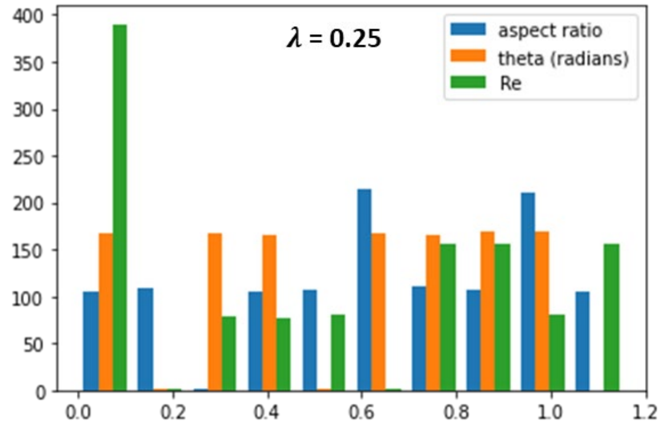

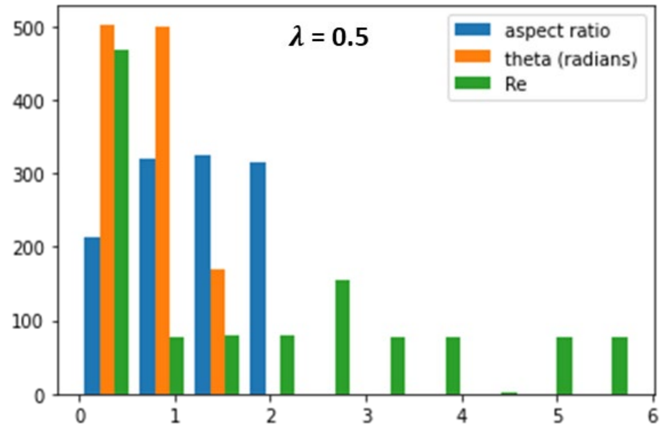

Neural Network Model for An Spherocylinder

Selected Neural Network Model

- Learning Rate – 0.001
- Batch Size – 32
- Epoch – 1000
- Cost Function –Mean Squared Logarithmic Error
- Activation Function (hidden layers) – ReLU

```
Model: "sequential_60"
_________________________________________________________________
 Layer (type)                 Output Shape              Param #
=================================================================
 dense_420 (Dense)            (None, 3)                 12

 dense_421 (Dense)            (None, 50)                200

 dense_422 (Dense)            (None, 150)               7650

 dense_423 (Dense)            (None, 350)               52850

 dense_424 (Dense)            (None, 500)               175500

 dense_425 (Dense)            (None, 350)               175350

 dense_426 (Dense)            (None, 50)                17550

 dense_427 (Dense)            (None, 3)                 153

=================================================================
Total params: 429,265
Trainable params: 429,265
Non-trainable params: 0
```

Table 5. MLNN Best Performance Results on Observed Data

Learning Rate	Batch Size	Layers	Train Time	RMSE	R^2 Cd	R^2 Cf	R^2 Cm
0.001	32	5	12m 57s	5.5	0.98	0.98	0.98

Table 6. MLNN Best Performance Results on Unobserved Data

Learning Rate	Batch Size	Layers	RMSE UD	R^2 UD Cd	R^2 UD Cf	R^2 UD Cm
0.001	32	5	2.1	0.99	0.88	0.94

Hyper Parameters	Values
Learning Rate	0.00005
	0.0001
	0.001
Layers	1
	5
	10
Batch Size	32
	225
	512

Neural Network Model for An Spherocylinder

Model Performance

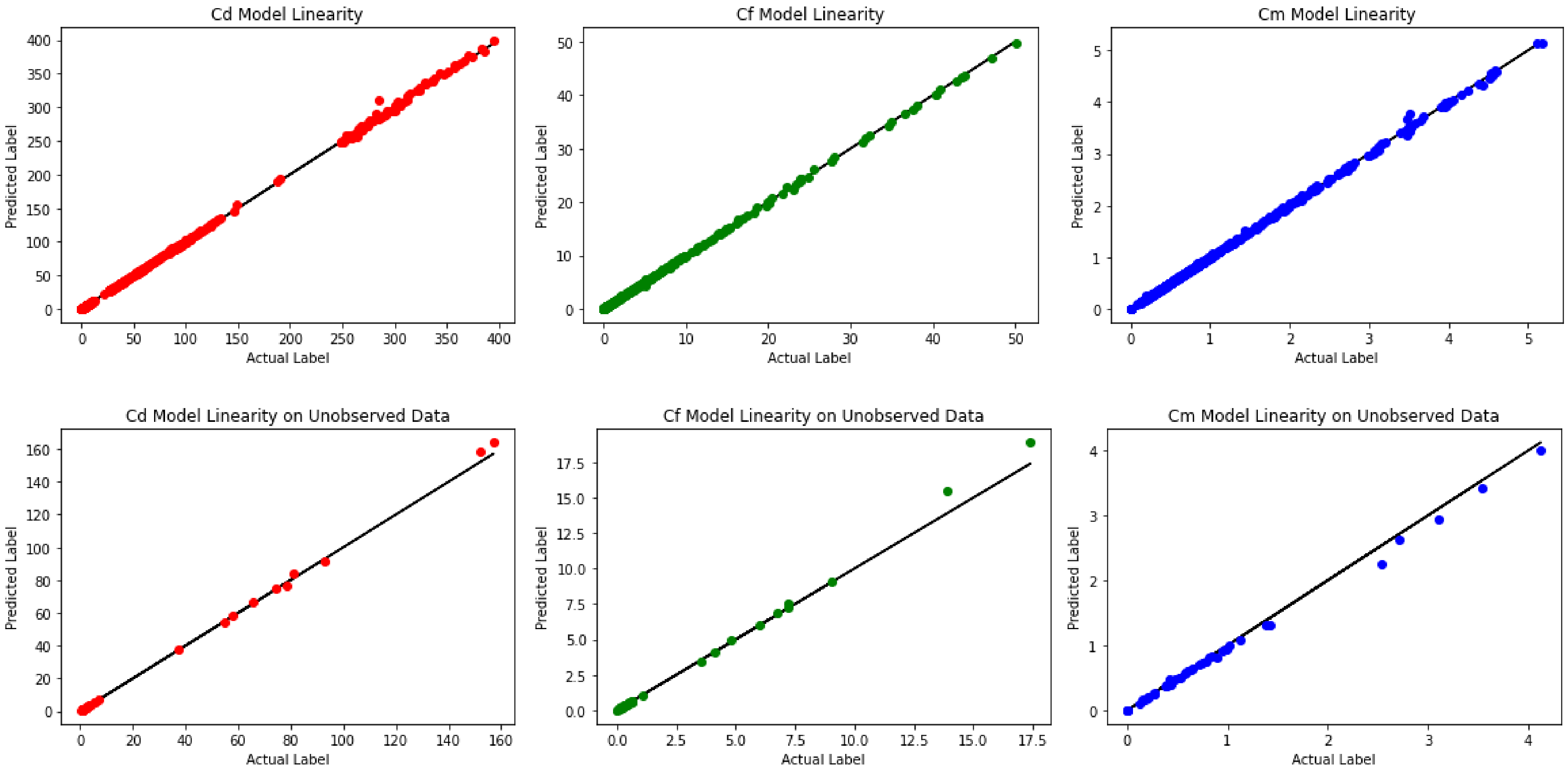

Neural Network Model for An Spherocylinder

Comparison with the correlation of drag correlations

- 1000 random cases for aspect ratio, incident angle, and Reynolds number
- MLNN achieved a correlation coefficient of 99.9%
- MLNN coefficient of drag estimates fit the correlation extremely well

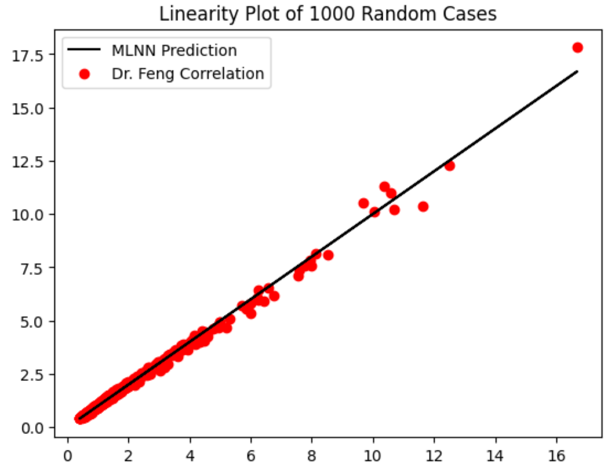

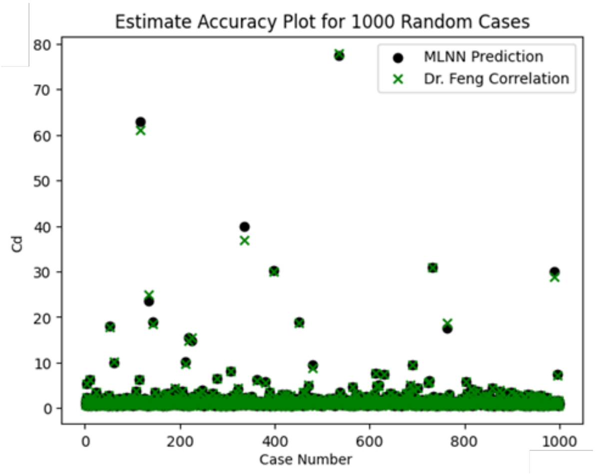

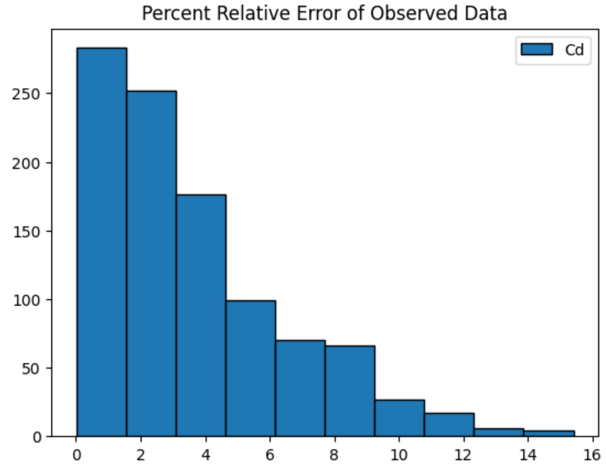

Artificial Neural Network Model for An Ellipsoid

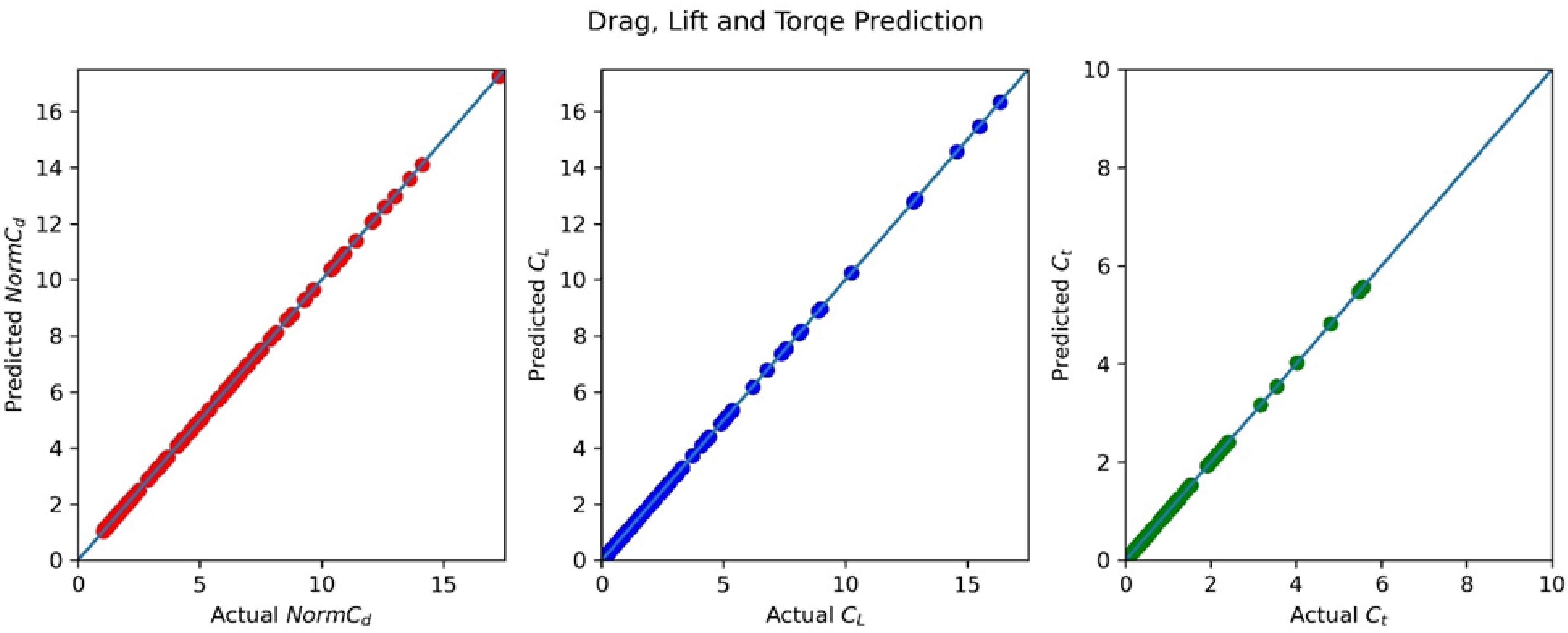

Artificial Neural Network Model for An Ellipsoid

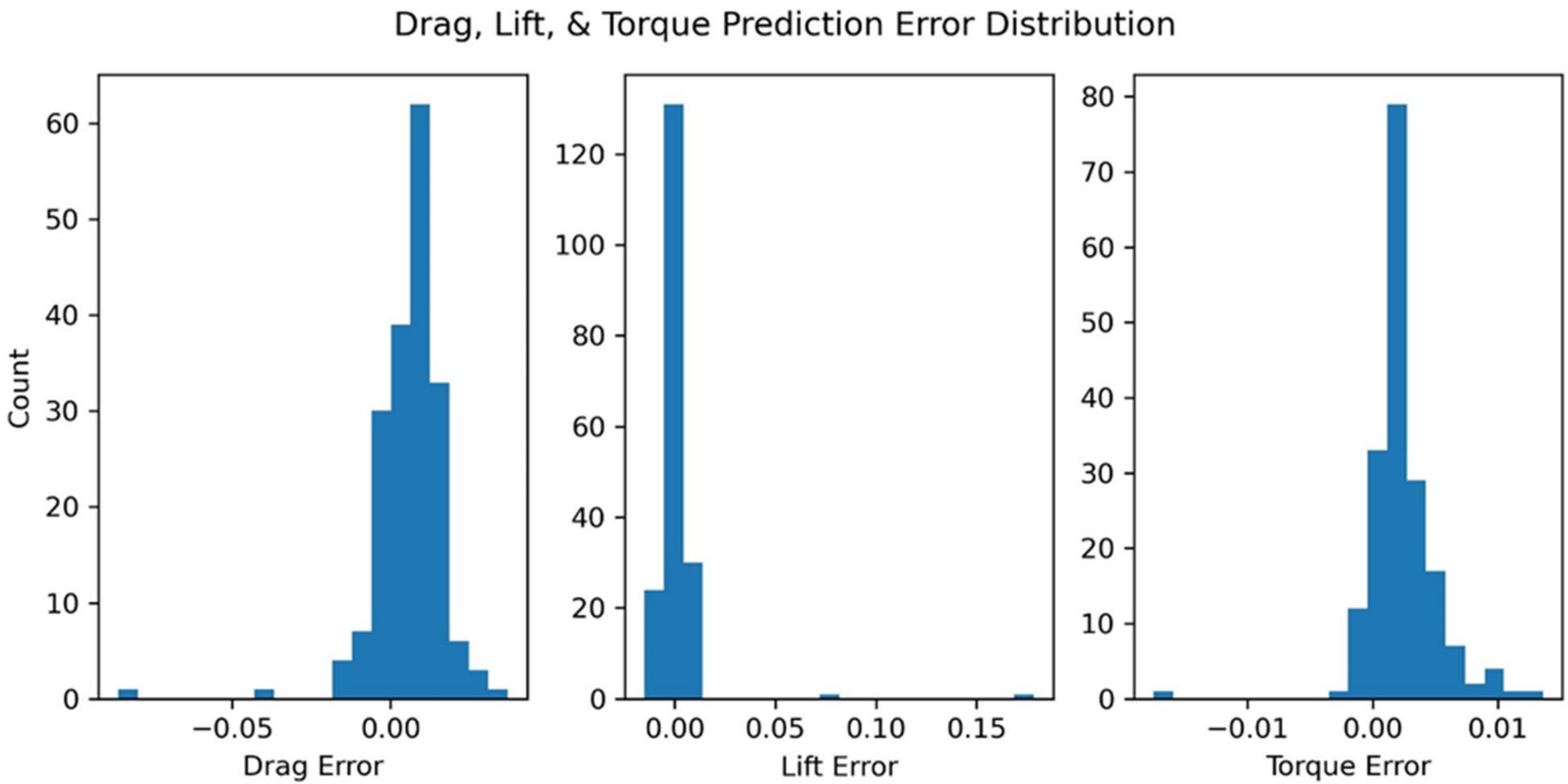

Artificial Neural Network Model for An Ellipsoid

DNS, ANN predictions, and present correlation comparisons

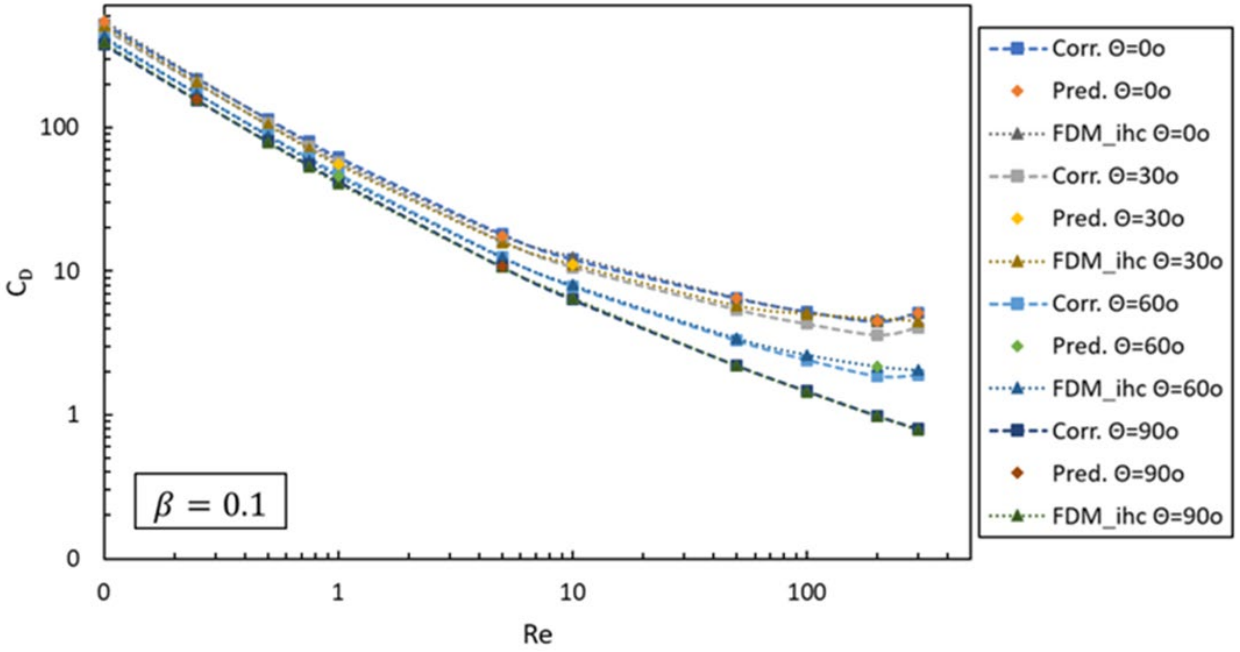

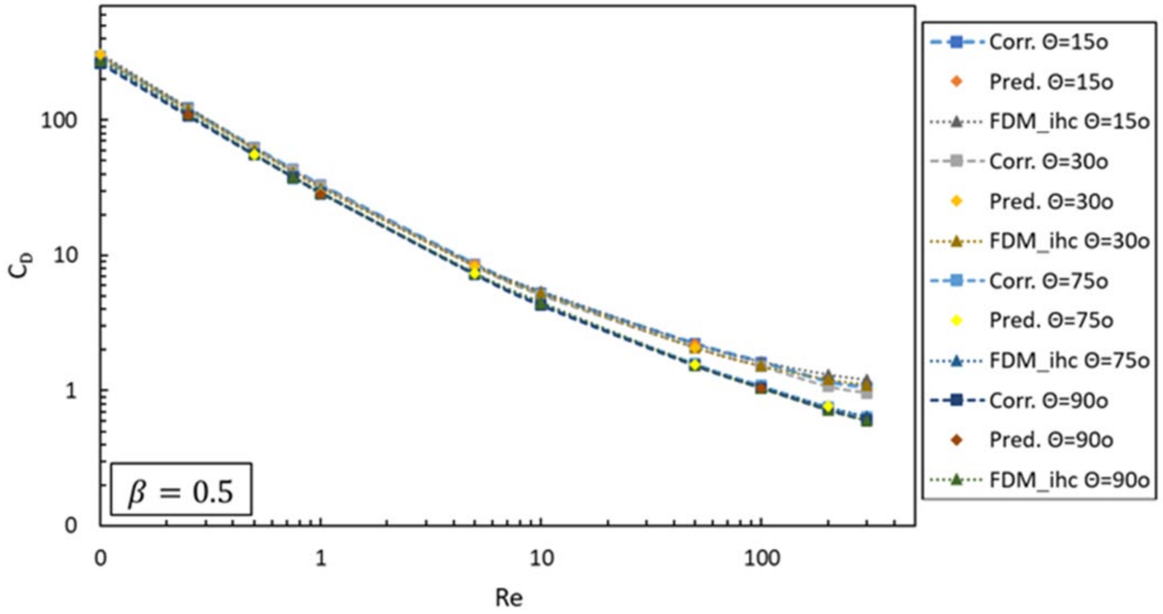

Drag model of an assembly of non-spherical particles

Additional input parameters

- Solid fractions
- Orientations at high solid fractions
- Mixture ratio of different shapes of particles

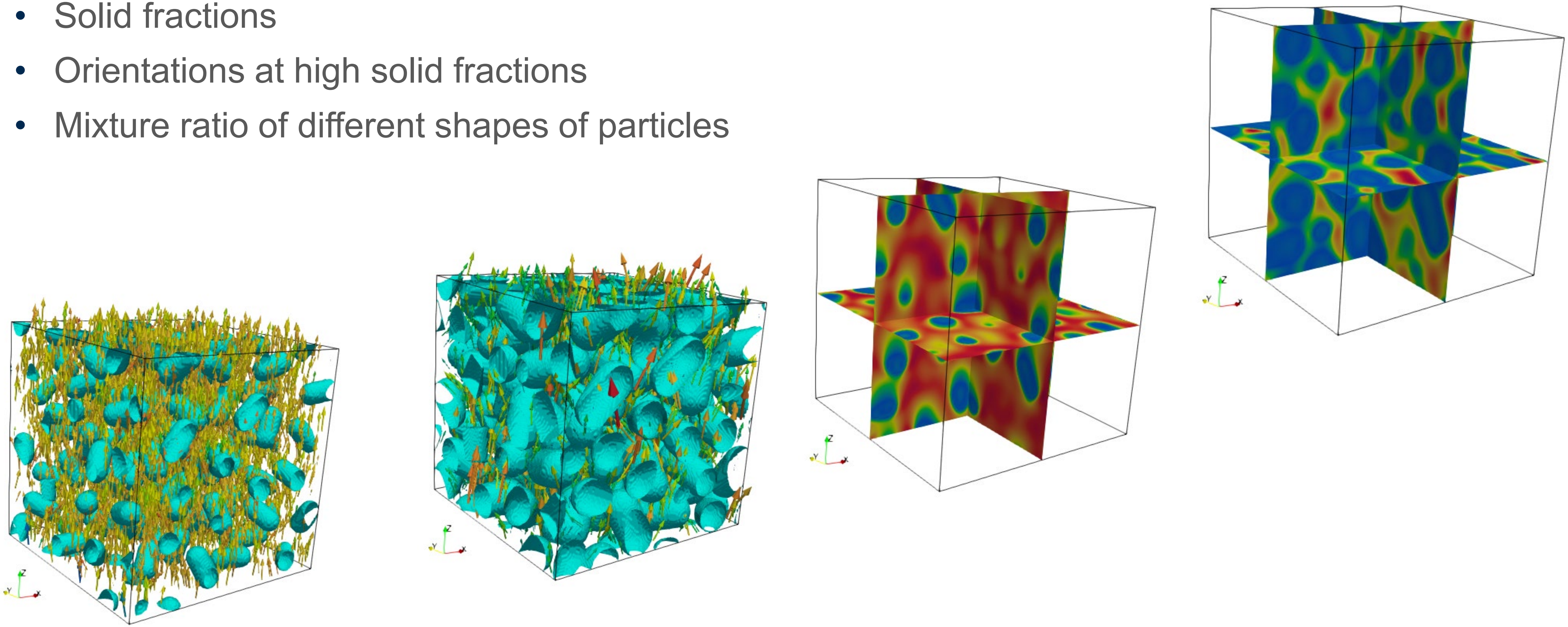

Assembly of Spheres: Validations

Stokes flow over an assembly of face-centered arrays of spheres.

Analytical solutions of Hashimoto (1959) for $\phi < 0.2$

Numerical solution of Sangani and Acrivos (1982)

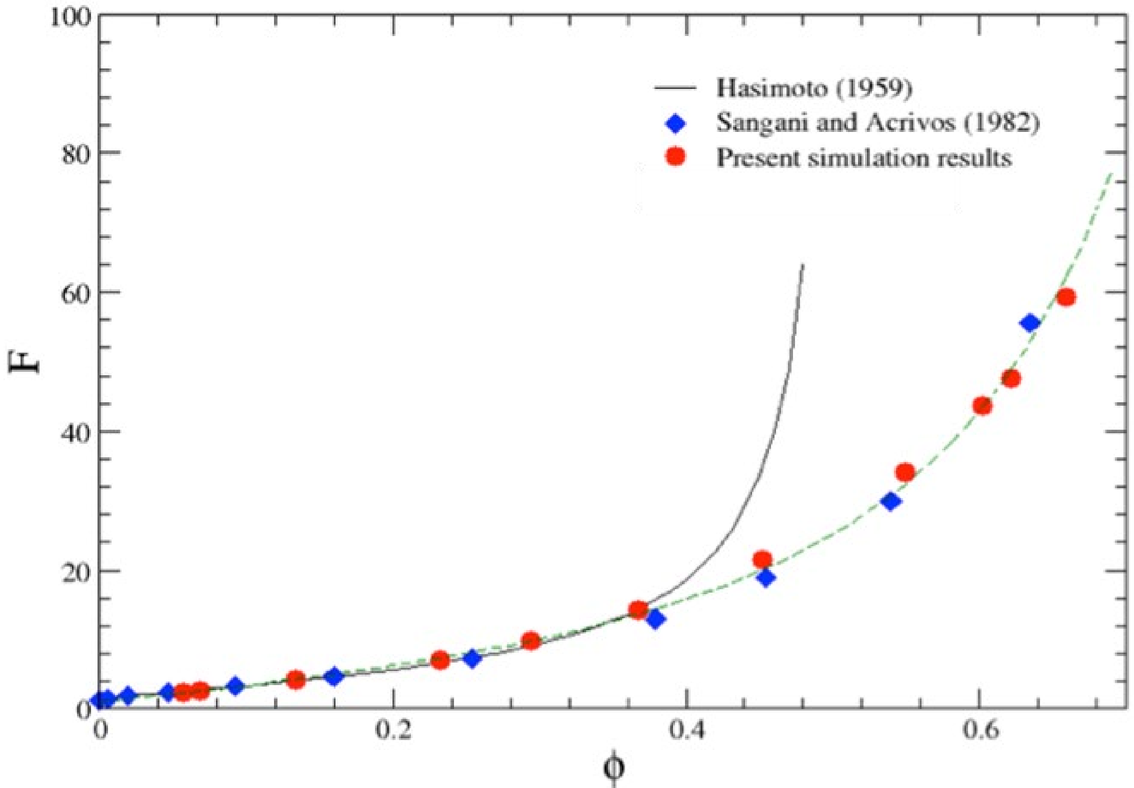

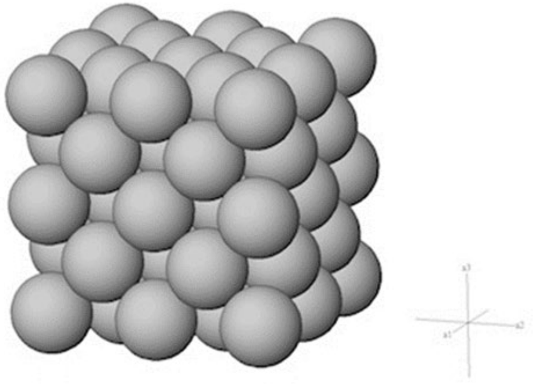

Dimensionless drag: $F = \dfrac{\boldsymbol{F}_d}{3\pi\mu d\boldsymbol{U}}$

Assembly of Spheres

Influence of different configurations at the same solid fraction and the same $\frac{dp}{dz}$

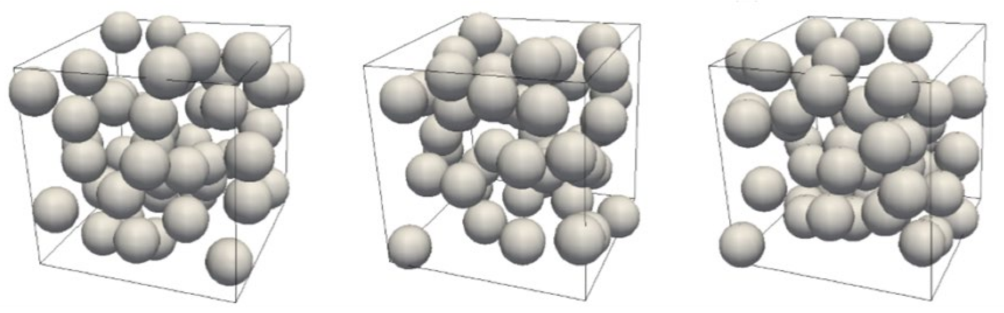

50 spheres at solid fraction $\phi = 0.287$

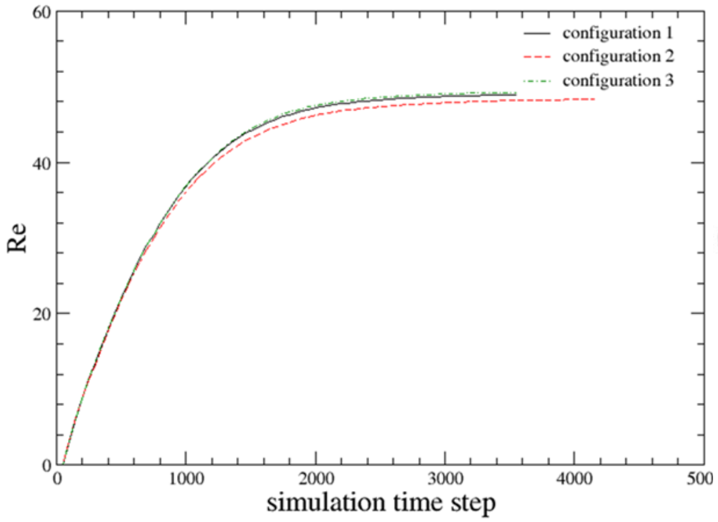

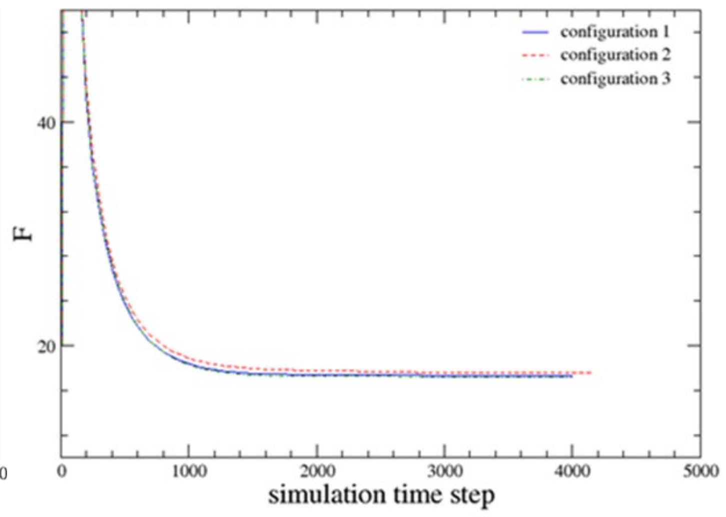

Influence of number of particles used in a simulation box for $\phi = 0.2$ and $Re = 56$

	Number of Particles	50	150	200
	Dimensionless Drag F	9.32	9.50	9.44

Drag model of an assembly of spheres

Ergun: $F^*(\phi, Re) = 150\phi/(18(1-\phi)^2 + 1.75/(18(1-\phi)^2\, Re$.

Wen and Yu: $F^*(\phi, Re) = (1 + 0.15Re^{0.687})(1-\phi)^{-3.7}$.

Tang et al. (2015):

- $F^*(\phi, Re) = \frac{10\phi}{(1-\phi)^2} + (1-\phi)^2(1 + 1.5\sqrt{\phi}) + \left[0.11\phi(1+\phi) - \frac{0.00456}{(1-\phi)^4} + \left(0.169(1-\phi) + \frac{0.0644}{(1-\phi)^4}\right)Re^{-0.343}\right]Re$.

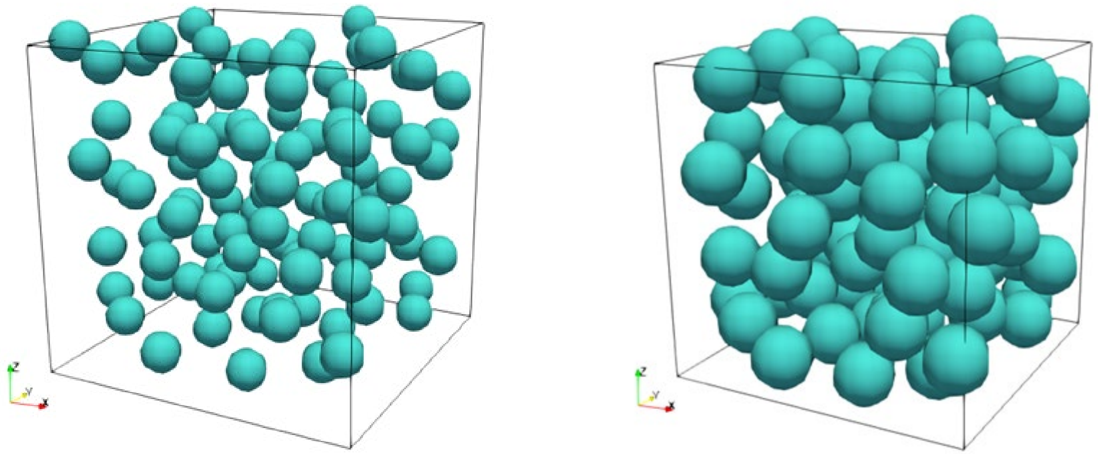

Random distributions of 100 spheres in a cube for $\phi = 0.1$ and $\phi = 0.4$.

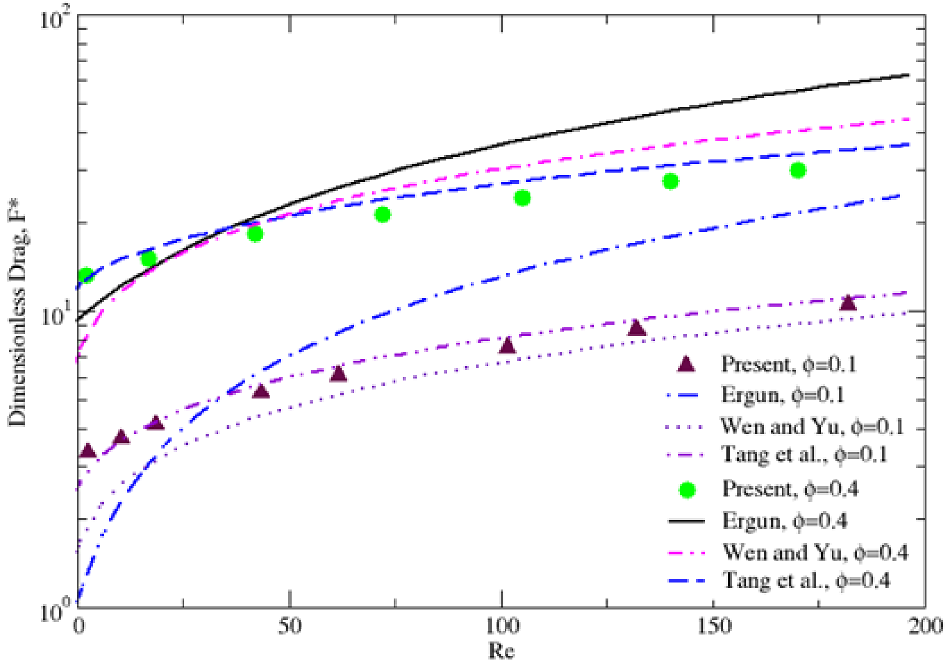

Individual drag force of 100 spherocylinders in an assembly

1.Individual drag forces fluctuate within approximately 10% of the average drag force.

2.The lift forces exerted on the particles are relatively insignificant when compared to the drag forces

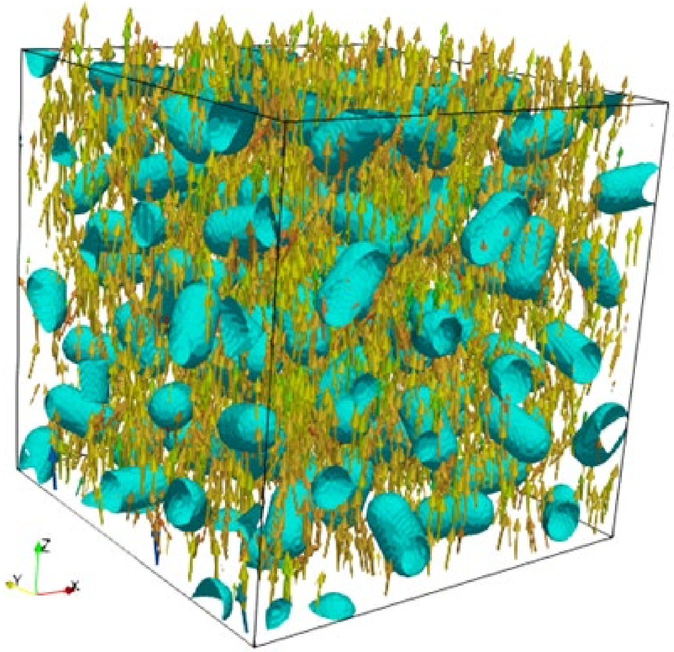

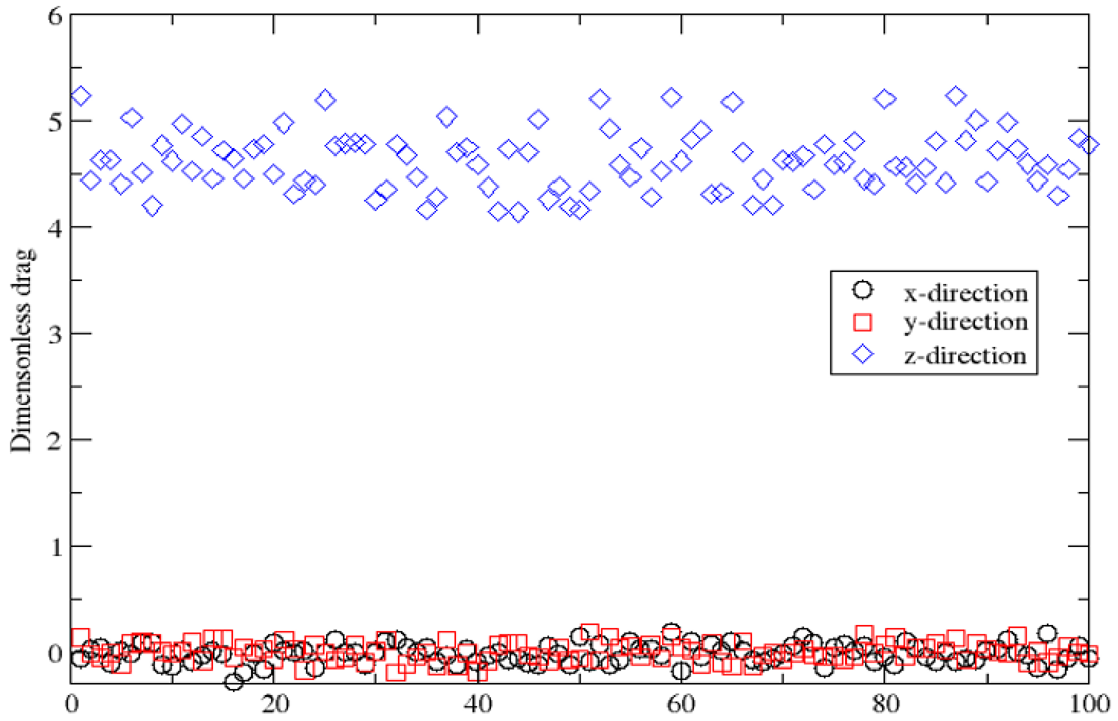

Dimensionless fluid-sphere forces of 100 particle at Re=18.3 and $\phi = 0.1$

Assembly of Spherocylinders

Effect of different configurations

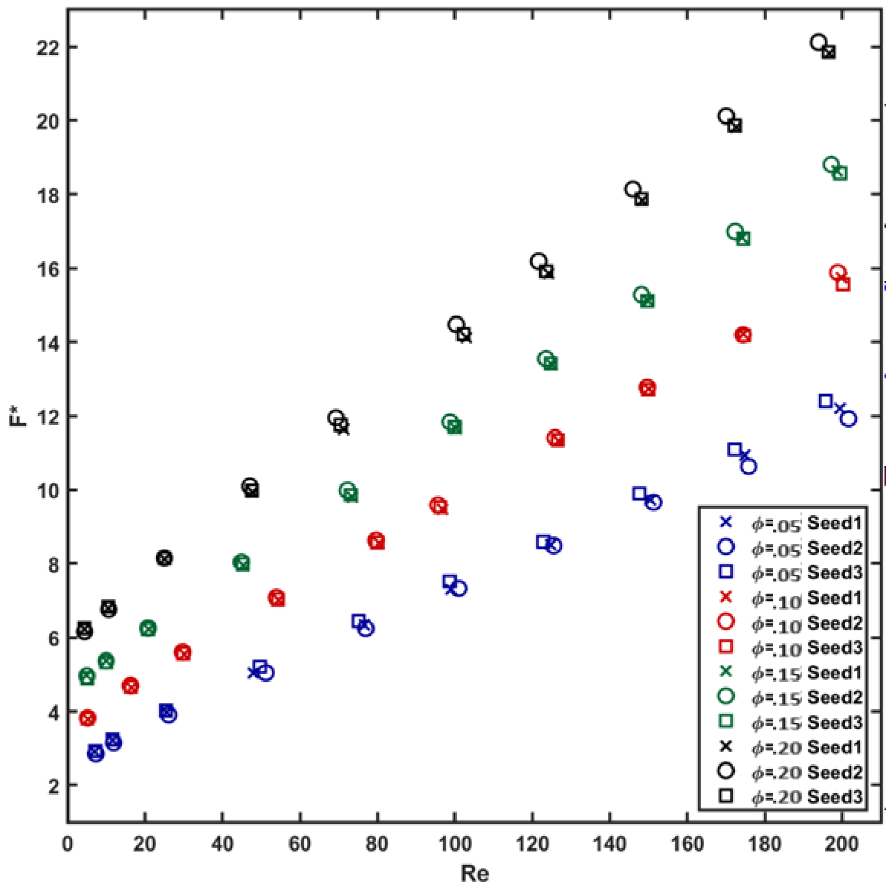

Comparison with sphere drag models

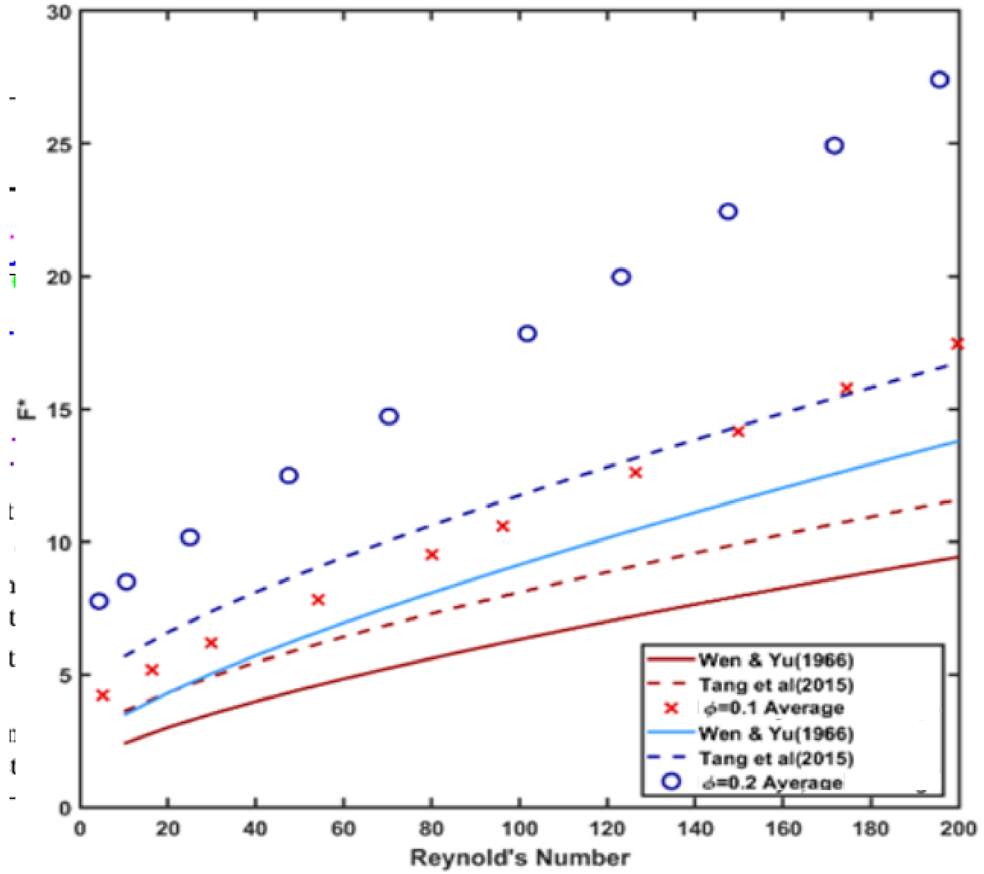

Assembly of Mixed Spheres and Ellipsoids

Average dimensionless drag of an assembly (80 particles) of mixed spheres and ellipsoids at solid fraction $\phi = 0.1$ at different mixed ratio

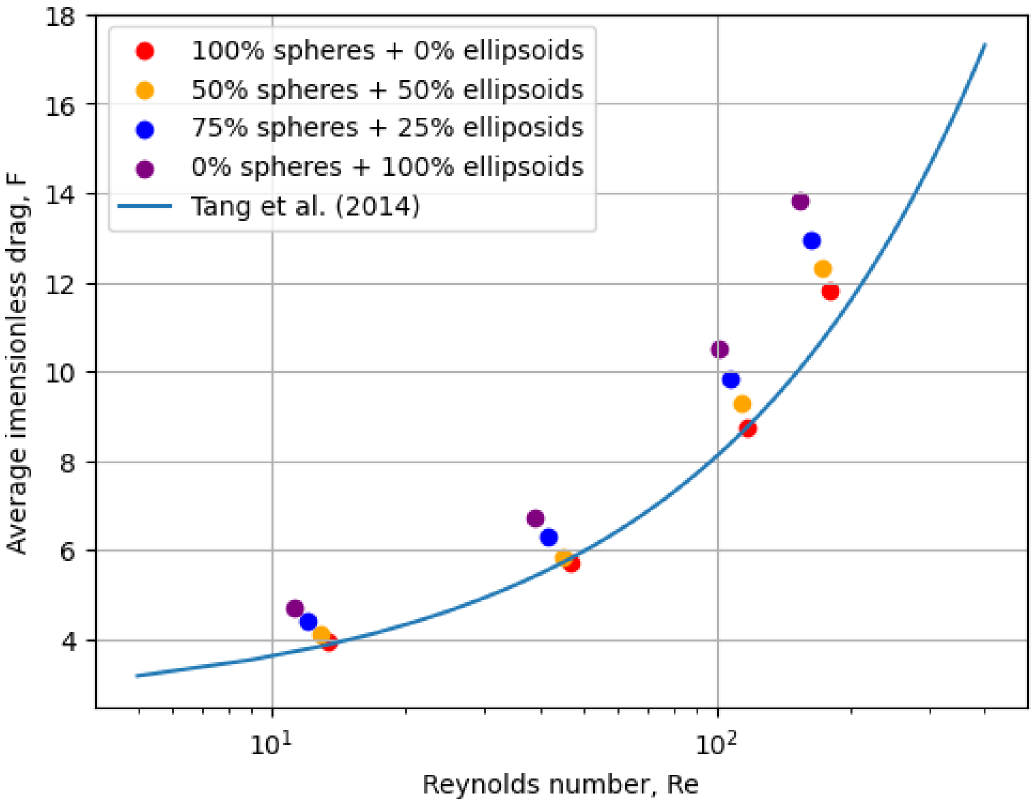

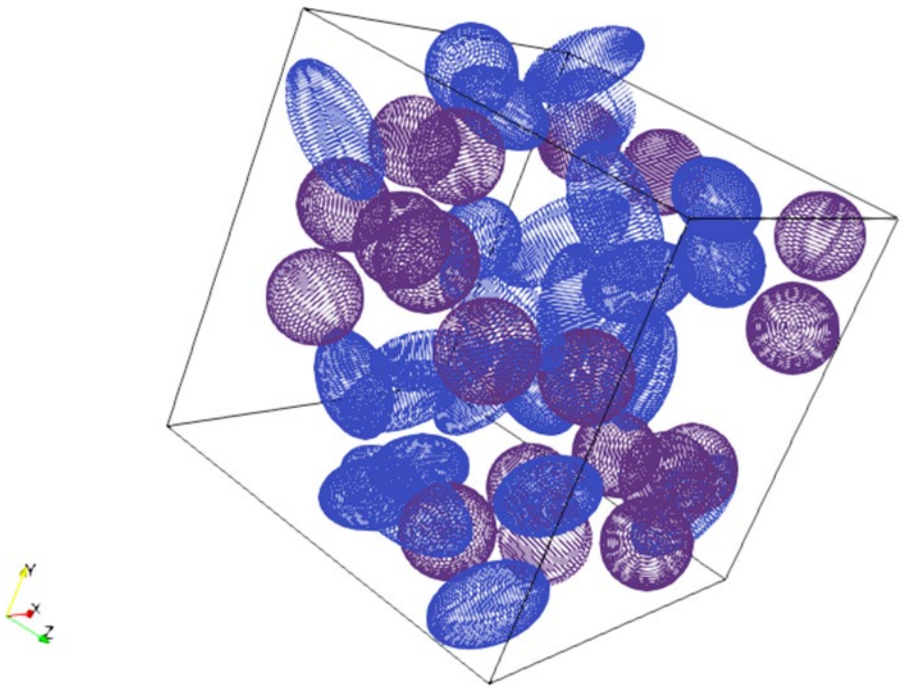

Assembly of Mixed Spheres and Ellipsoids

Average dimensionless drag for spheres and ellipsoids:

Percentage of ellipsoids	Re	Average F for all particles	Average F for spheres	Average F for ellipsoids
0%	179	11.83	11.83	N/A
25%	175	12.13	11.45	14.16
75%	163	12.96	11.42	13.47
100%	153	13.84	N/A	13.84

1. At the same pressure gradient, Reynolds number decreases as the percentages of nonspherical ellipsoids increases.

2. The average drag for spheres is less than that for ellipsoids, i.e., no-spherical particles would have higher drag coefficients in comparison with spheres

Current and Future Work

Neural Network Model for the drag coefficients of assemblies of particles

Non-spherical particles:

  spherocylinders, ellipsoids, and mixed bi-disperse assembly

Input parameters:

  Reynolds number, aspect ratio, solid fraction, orientation, bi-disperse mixed ratio

Acknowledgments

Student contributors to this project

- Graduate students: Joshua Corner, Daniel Hinojosa, Sergio Molina, Miguel Cortina, Jack Smith, and James Standard.
- Undergraduate student: Andres Leon Islas, Mahnoor Bokhari, James Moseley, and Joshua Beltran

Journal Publications:

"Wall Effects on the Flow Dynamics of a Rigid Sphere in Motion." Journal of Fluids Engineering 143, no. 8 (2021): 081106.

"Review—Drag Coefficients of Non-Spherical and Irregularly Shaped Particles." ASME. J. Fluids Eng. June 2023; 145(6): 060801.

"A general and accurate correlation for the drag on spherocylinders." International Journal of Multiphase Flow 168 (2023): 104579.

Thank you for your time and attention!